Fibronectin Molecule Visualized in Electron Microscopy: A Long, Thin, Flexible Strand

HAROLD P. ERICKSON, NADIA CARRELL, and JAN McDONAGH
Department of Anatomy, Duke University Medical Center, Durham, North Carolina 27710, and Department of Pathology, University of North Carolina, Chapel Hill, North Carolina 27514

ABSTRACT We have determined the structure of plasma fibronectin by electron microscopy of shadowed specimens. The 440,000 molecular weight, dimeric molecule appears to be a long, thin, highly flexible strand. The contour length of the most extended molecules is 160 nm, but a distribution of lengths down to 120 nm was observed, indicating flexibility in extension as well as in bending. The average diameter of the strand is 2 nm and there are no large globular domains. The large fragments produced by limited digestion with plasmin are not globular domains but are segments of the strand, whose length corresponds to the molecular weight of the polypeptide chain. We conclude that each polypeptide chain of the dimeric molecule spans half the length of the strand, with their carboxyl termini joined at the center of the strand and their amino termini at the ends. This model is supported by images of fibronectin-fibrinogen complexes, in which the fibrinogen is always attached to an end of the fibronectin strand.

Fibronectin is a high molecular weight glycoprotein that is found in a soluble form in blood and other extracellular tissue fluids, and in an insoluble form in connective tissues and attached to cell surfaces. Fibronectin is thought to mediate the attachment of cells to the other components of the extracellular matrix, in particular to collagen and, where it occurs, fibrinogen or fibrin (for reviews see 14, 16, 22, 26). Both plasma fibronectin and the cell surface or extracellular matrix forms are dimers, comprising two subunits of 220,000 mol wt, covalently linked by a single disulfide bond near their carboxyl termini. The two polypeptide chains are identical by most criteria but are frequently separated as a closely spaced doublet in gel electrophoresis; the basis for this separation is not known (11). Cell surface fibronectin differs from plasma fibronectin in carbohydrate content and solubility and exists as oligomers of the basic dimeric molecule, but the two forms are very similar in amino acid composition and are immunologically indistinguishable (14).

Plasma fibronectin has a sedimentation coefficient of 8 to 13S, depending on the pH and ionic strength (1). This is too small for a globular protein of 440,000 mol wt, and suggests that the molecule has an elongated shape (1). Studies with proteases have shown that fibronectin can be cleaved into a number of large fragments or domains, and it has been found that the different binding functions are retained by the separated domains. By analogy with the well established trinodular structure of fibrinogen, it has been suggested (1, 16) that fibronectin may have a nodular structure, consisting of large globular domains connected by flexible linking segments that can be readily attacked by proteases.

Techniques of electron microscopy are now well established for determining the structure of large proteins. Molecular structures determined from shadowed specimens include the globular heads and the thin rodlike tail of myosin (3, 21), the thicker, more flexible strands of spectrin (17, 21) and actin binding protein (20), and the trinodular structure of fibrinogen (5). Because these techniques clearly reveal and distinguish between thin, elongated structures and larger globular domains, they seemed ideally suited for studying the structure of fibronectin.

MATERIALS AND METHODS

Fibronectin was prepared from fresh-frozen, cryoprecipitate-poor, human Cohn fraction I (4). Trasylol, benzamidine, EDTA, and episilon-aminocaproic acid were used throughout the purification procedure. Cohn fraction I was diluted in 0.15 M NaCl, 0.1 M sodium phosphate buffer, pH 7.2, containing the inhibitors, and was adsorbed onto gelatin-Sepharose. The adsorbed material was washed, sedimented, and resuspended four times and then packed into a column. The column was washed with buffer containing 1 M NaCl and the fibronectin was eluted with buffer containing 4 M urea and quickly dialyzed into buffer without urea. The entire purification was carried out at room temperature.

Fragments of fibronectin were prepared by digestion with plasmin (Kabi, Stockholm, Sweden.) at 0.5 CU/mg fibronectin for 45 min at 37°C in 0.05 M Tris, 0.1 M NaCl, pH 8.6. The reaction was stopped with Trasylol and the

THE JOURNAL OF CELL BIOLOGY · VOLUME 91 DECEMBER 1981 673-678

fragments were separated by chromatography on gelatin-Sepharose. The nonbinding fragments were eluted with Tris-saline, and the bound fragments were eluted with the same buffer containing 4 M urea. Both fractions were dialyzed against 0.02 M Tris, 0.1 M NaCl, 4 mM EDTA, pH 7.2, and samples were removed for electron microscopy.

Gel electrophoresis in 0.1% SDS was performed on 5% and 3.75% polyacrylamide gels as previously described (12). Molecular weights were calculated by reference to proteins in calibration kits from Pharmacia Fine Chemicals (Piscataway, N. J.). Gel analysis of the purified fibronectin and fragments are shown in Fig. 1.

Shadowed specimens were prepared for electron microscopy using the procedures developed previously for visualizing fibrinogen (5; see also reference 21 for a discussion of the effect of different salts in the buffer). Protein was diluted to a concentration of 0.01–0.04 mg/ml in a buffer containing 40% wt/vol glycerol and 0.25 M ammonium formate, pH 7, and a small quantity of this solution was sprayed onto pieces of freshly cleaved mica. The samples were shadowed with platinum-carbon (90:10 Pt:C) at an angle of ~ 10 degrees for unidirectional shadowing, or 5 degrees for rotary shadowing.

Micrographs were taken on a Philips EM 301 electron microscope at a nominal magnification of 40,000 times. Magnification was calibrated from micrographs of negatively stained tropomyosin paracrystals (17) and catalase crystals (25). The magnification determined from either standard was reproducible to about 1%, but the two standards consistently disagreed by about 4%. A compromise magnification was therefore selected at which the tropomyosin periodicity was 38.8 nm (instead of 39.5 nm) and the catalase periodicity was 17.7 nm (instead of 17.2 or 17.5 nm). Prints of the fibronectin images were made at a total magnification of 150,000 times and the lengths of individual molecules were measured with a Numonics 1224 Electronics Graphics Calculator (Numonics Corp., Lansdale, Pa.)

RESULTS

Images of typical fields of fibronectin are shown at low magnification in Fig. 2, and selected molecules are shown at high magnification in Fig. 3. Preparations containing some copurifying fibrinogen were preferred for the electron microscopy because the trinodular fibrinogen molecules are easily recognized in both the unidirectional- and rotary-shadowed preparations, and they are useful as an internal structural reference. The nodular fibrinogen molecules were very rare in the preparations of highest purity (Fig. 1 *b*), but could be 5 to 10% as numerous as fibronectin in preparations showing a comparable amount of fibrinogen on SDS gels.

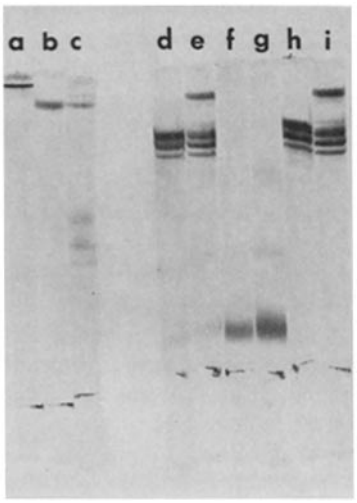

FIGURE 1 Polyacrylamide gel electrophoresis of fibronectin and the fragments from plasmin digestion. Gels *a–c* are 5%, and *d–i* are 3.75% polyacrylamide. *a*, *b*: purified fibronectin, nonreduced and reduced. *c*: fibronectin with copurifying fibrinogen, indicated by the three subunits of lower molecular weight. *d*, *e*: plasmin digest of fibronectin, reduced and nonreduced. *f*, *g*: the non-gelatin-binding fraction from the plasmin digest, reduced and nonreduced. *h*, *i*: the gelatin binding fraction from the plasmin digest. The reduced fibronectin subunit appears as a closely spaced doublet, of average mol wt 220,000 (*b*, *c*). The three high mol wt bands in the plasmin digest (*d*) correspond to mol wt ~ 220,000 (mostly undigested fibronectin, but also containing some fragments of 210,000), 190,000, and 180,000. The high mol wt band in *e* is the nonreduced and undigested fibronectin dimer. The nonbinding fragments in *f*, *g* are 30,000 subunit mol wt, with a faint band of 60,000 in the nonreduced sample; smaller peptides are not seen on these gels. The gelatin binding fraction (*h*, *i*) contains only the high mol wt fragments and undigested fibronectin.

The fibronectin molecules are thinner and much longer than fibrinogen and are irregularly extended and bent. Well extended molecules appear remarkably uniform in thickness, and there are no globular domains comparable to those of fibrinogen. This is indicated by the uniformity of the shadow boundary in the unidirectional-shadowed molecules, rows *a* and *b*, (Fig. 3) which may be contrasted with the longer triangular shadows of the fibrinogen nodules (row *b*, 4–6). The uniform thin strand of fibronectin is more clearly demonstrated and contrasted to the nodular structure of fibrinogen in the rotary-shadowed preparations, rows *c* through *e* (Fig. 3).

Two structural features were observed with some consistency. The first is an elaboration of one or both ends into a forklike structure (see, for example, row *c*, 5–6, and row *d*, 1–3 of Fig. 3). We note also that some of the images of actin binding protein presented by Tyler et al. (20) show a very similar forked end. The fork could be a random kink at the end of the strand, or it may be a more permanent feature of tertiary structure. The second structural feature, which is observed less frequently, is a segment of 10 to 30 nm, usually near the center of the strand, that appears to be missing. These "missing" segments might be produced if the molecule had an ellipsoidal profile over some segments that is poorly visualized by the shadowing when flat on the mica, or the strand may be stretched thin or broken at these points.

Molecules were selected for length measurement if they were sufficiently well extended so that the contour could be traced with reasonable confidence. Molecules that were tangled were not measured and, in the measurements of the native fibronectin, the small fraction of very short fragments and globular particles was ignored. A histogram of lengths of 120 rotary-shadowed molecules showed a fairly uniform distribution of lengths from 120 to 160 nm (Fig. 5 *a*). We believe that the spread in the measured lengths can be attributed only partially to ambiguity in tracing the contour of the molecules, and probably reflects a real variation in the extension of different molecules. The average length of 140 nm is perhaps less meaningful than the 160 nm length of the most extended molecules. The shorter molecules may be kinked or folded back over segments too small to resolve in the shadowed specimens, or they may be more tightly folded at points of flexibility.

The thickness of the fibronectin strands can be roughly estimated as 2 to 3 nm by measuring the shadow length of unidirectional-shadowed molecules or their apparent thickness in rotary-shadowed specimens. The average thickness can be estimated more precisely by calculating the volume that the protein must occupy and dividing by the length to obtain the average cross sectional area. For a partial specific volume of 0.73 cm^3/g the 440,000 mol wt protein will occupy a volume of 533 nm^3. For a length of 160 nm the average diameter is calculated to be 2.0 nm.

In the samples that we examined by electron microscopy, which generally contained some contaminating fibrinogen,

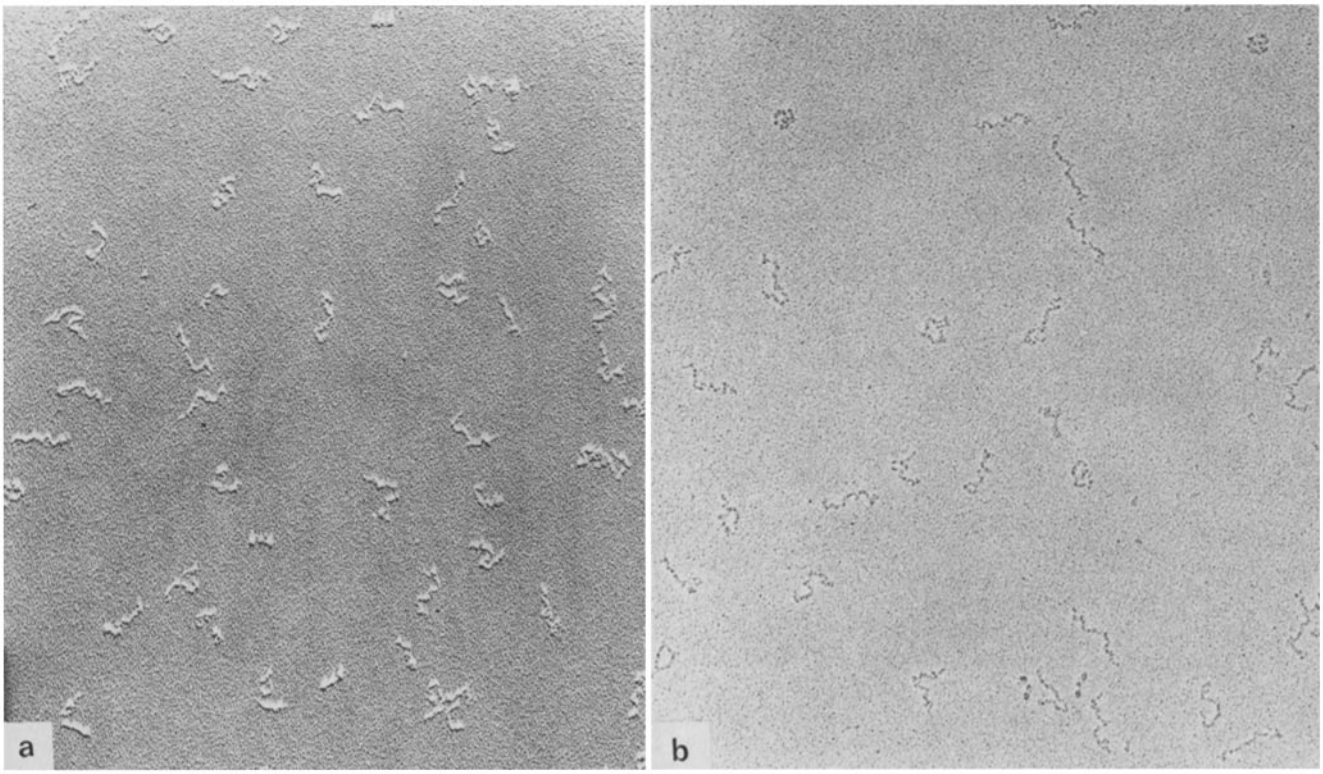

FIGURE 2 Fields of fibronectin molecules, with some copurifying fibrinogen, as seen in unidirectional shadowing (*a*) and rotary shadowing (*b*).

instances of fibronectin strands attached to fibrinogen molecules were found consistently. Five examples are shown in Fig. 3, row *e*. The attachment was always at an end of the fibronectin strand, and in most cases the fibronectin was attached to an end nodule of the fibrinogen. In some preparations a significant number of complexes were found in which the fibronectin was attached to the middle nodule of fibrinogen (Fig. 3 *e4*). Occasional complexes had a fibrinogen at each end of the fibronectin (Fig. 3 *e5*).

It is known that fibronectin binds to fibrinogen and can be crosslinked by Factor XIIIa to a segment near the amino terminus of the fibronectin subunits (15, 24). The crosslink acceptor site on fibronectin has been identified as a glutamine, three residues from the amino terminus (13). The fibrinogen-fibronectin complexes are almost certainly linked covalently because an association constant $> 10^7\ M^{-1}$ would be required to prevent dissociation in the dilute solution used for sample preparation. The association of fibronectin and fibrinogen must be much weaker than this or they would precipitate in the blood. We believe the complexes may have been produced by an endogenous Factor XIIIa activity. This interpretation is suggested by the presence of fibrinogen dimers in the same preparations (Fig. 3: *b6*, *d5*, and *e3, 5*), which closely resemble the "end-to-end" fibrinogen dimers that we have prepared in vitro by crosslinking with Factor XIIIa (6). There was no detectable Factor XIIIa activity in the final fibronectin preparations, so we assume the fibrinogen dimers and the fibronectin-fibrinogen complexes were present in the plasma or were formed by an endogenous transglutaminase activity during the early stages of purification. Experiments are now in progress to confirm the existence of a covalent crosslink and to identify the chains of fibrinogen involved in the different complexes. The important conclusion at present is that the fibrinogen attachment at the end of the fibronectin strand strongly suggests that this is the location of the amino terminus.

Plasmin digestion is known to cleave the fibronectin subunits into a large core fragment and some smaller fragments (14). The core fragments are missing the carboxyl terminal segment that contains the interchain disulfide bond, so they are no longer covalently linked. The limited plasmin digestion in our experiment produced a family of high molecular weight core fragments from 180,000 to 210,000 subunit mol wt, as well as 30,000 mol wt fragments and smaller peptides not seen on the gels (Fig. 1). Comparison of the reduced and nonreduced gels shows a small fraction of undigested dimeric molecules, and demonstrates that all of the high molecular weight fragments are missing the interchain disulfide bond.

The high molecular weight fragments retained the collagen binding site and could be separated from the other fragments by gelatin-Sepharose chromatography. Micrographs of native fibronectin, the high molecular weight collagen binding fragment, and the smaller, nonbinding fragments are shown in Fig. 4. A histogram of the lengths of the fragments is given in Fig. 5. Only 13% of the collagen binding fraction had a length > 110 nm. This corresponds closely to the fraction of native fibronectin in this sample as determined by gel electrophoresis (Fig. 1 *i*, and densitometer scans not shown). The more extended strands of this large fragment had a length of 65 nm. The mass per unit length of these fragments is essentially identical to that of the native molecule, assuming each 65-nm fragment comprises a single polypeptide chain of 190,000 mol wt, whereas the 160-nm native molecule comprises two chains of 220,000 mol wt each. This demonstrates that the native molecule does fall apart into halves, even under nondenaturing conditions, when the disulfide bonded central segment is cleaved out.

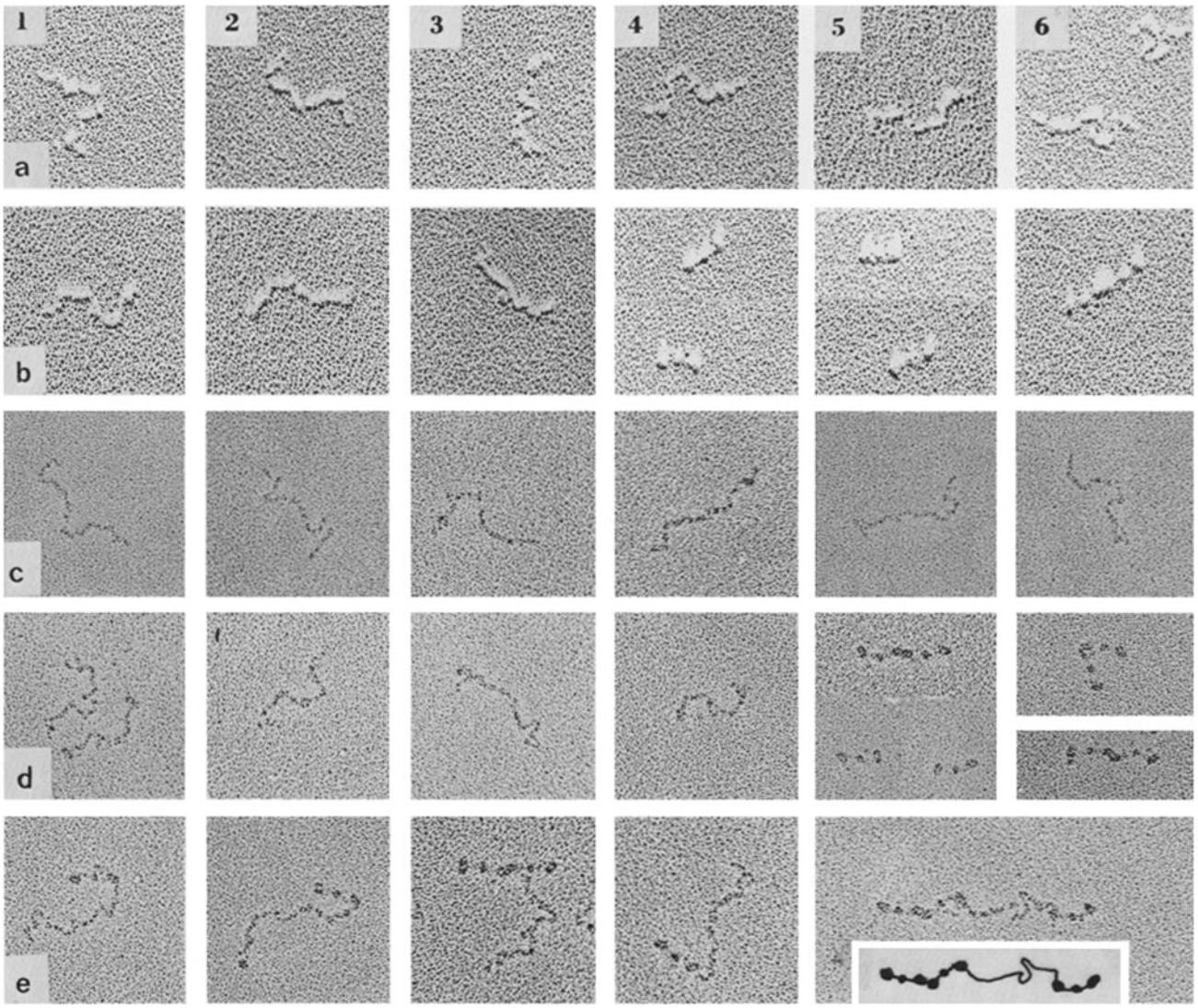

FIGURE 3 Selected examples of fibronectin molecules and of fibrinogen molecules and dimers found in the same preparations. Rows *a* and *b* are unidirectional- and rows *c*–*e* are rotary-shadowed. Row *a 1–6*, *b 1–3*: fibronectin molecules arranged in order of decreasing length, from 160 to 120 nm. Row *b 4* and *5*: fibrinogen molecules showing characteristic trinodular structure, and *b 6*: a fibrinogen dimer. Row *c 1–6*, *d 1–4*: fibronectin molecules ranging in length from 160 to 115 nm. Row *d 4* and *5*: fibrinogen molecules and dimers. Row *e 1, 2, 4*: fibronectin molecules attached to the outer nodules of fibrinogen. *e 3*: a fibrinogen dimer with a fibronectin attached to one of the central nodules. *e 5* a fibronectin strand with a fibrinogen dimer attached on its left end and a fibrinogen molecule on its right end (an interpretive drawing is given below the image). × 150,000.

A number of different preparations of fibronectin and different solution conditions were investigated. The appearance of the strands was unchanged if the salt concentration was varied from 0.5 to 500 mM, or if 10 mM calcium or EDTA was added to the buffer. Raising the pH from 7 to 9.5 had no effect, but at pH 4 the strands were more tightly coiled and were difficult to trace. In one experiment the fibronectin was further characterized and purified by zone sedimentation through a 15% to 40% glycerol gradient in 0.25 M ammonium formate, pH 7. The protein sedimented as a single peak with a sedimentation coefficient of 10S, which is close to the value of 10.8S previously determined in 0.4 M KCl (1). The strands from this 10S fraction were indistinguishable from those in the sample before sedimentation. Finally we examined a preparation of fibrinogen that was known from gel electrophoresis to contain a small amount of fibronectin. Typical fibronectin strands were found, so we conclude that the structure is not an artifact of the urea elution used in the normal preparation.

DISCUSSION

Two previous electron microscope studies of fibronectin have given conflicting and problematical interpretations. Vuento et al. (23), using the negative stain technique, obtained some intriguing images of fibronectin polymers showing linear strands and bundles. The protein concentration used for specimen preparation (0.5 mg/ml) was, however, much too high for visualizing single molecules (5). The coiled threadlike structures observed in that study were probably overlapping fragments of aggregated molecules. In another study fibronectin was shadowed after freeze-drying (10), and globular particles ~ 15 nm long by 9 nm wide were identified as single molecules. We cannot explain the origin of these structures, but in this study also the protein concentration was relatively high and it is difficult to identify individual molecules with confidence. In contrast, the specimens we describe here show a homogeneous population of well-separated, long, flexible strands, which can

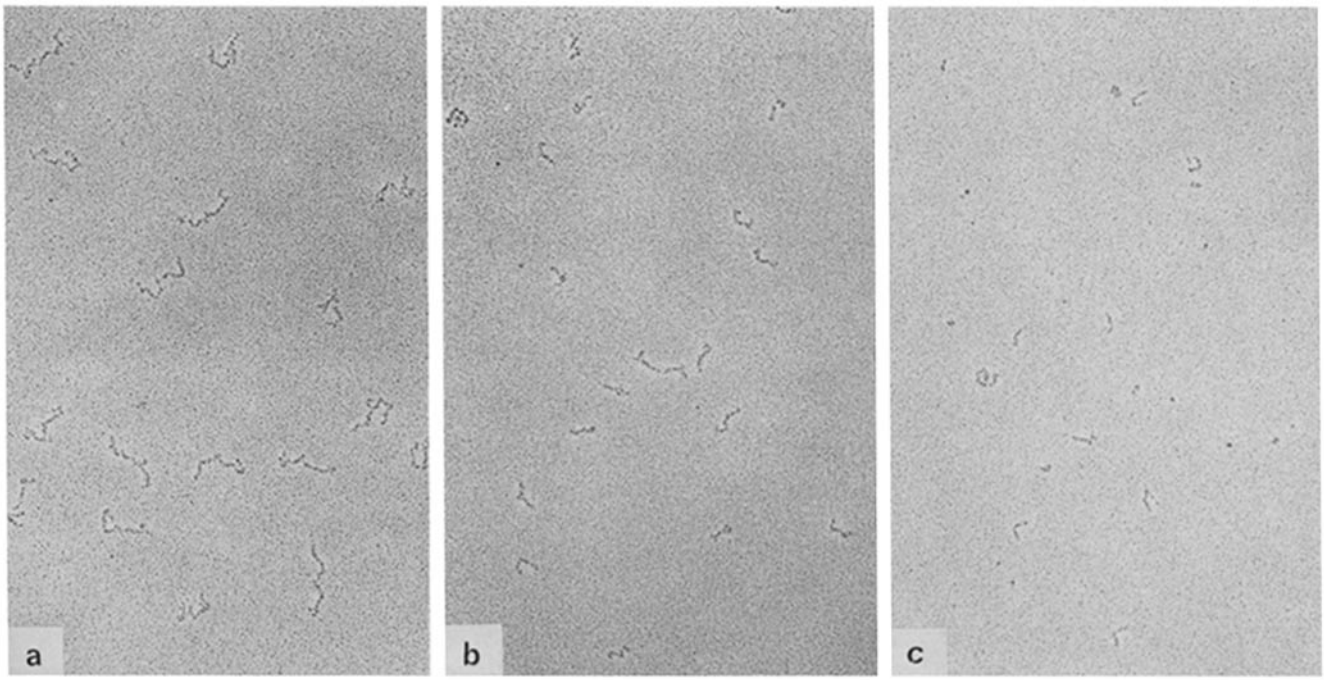

FIGURE 4 Micrographs of rotary shadowed fibronectin and plasmic fragments. *a*: Native fibronectin molecules. *b*: The high mol wt fragments that bound to the gelatin-Sepharose column. *c*: The smaller fragments that did not bind to the gelatin-Sepharose.

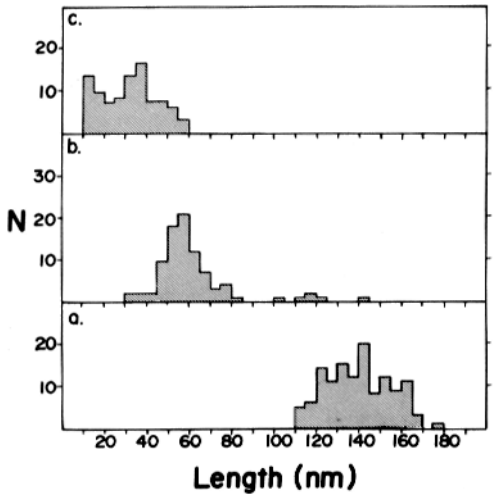

FIGURE 5 A histogram of lengths of (*a*) native fibronectin molecules, (*b*) the high mol wt gelatin binding fragment, and (*c*) the smaller, nonbinding fragments.

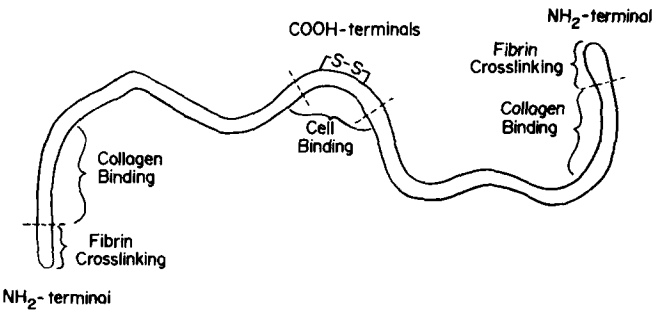

FIGURE 6 A model of the fibronectin molecule. The major plasmin cleavage sites are indicated by dotted lines, but we have not attempted to account precisely for the multiple cleavage sites that produce the family of high mol wt peptides. The molecule is drawn to scale based on our images, 160 nm long by 2 nm thick.

be identified confidently as individual molecules of fibronectin. The presence of the easily recognized fibrinogen molecules in some preparations served as an internal control to confirm that we were visualizing individual molecules.

In previous schematic diagrams mapping the functional domains obtained by limited proteolysis, the two polypeptide chains of the dimeric molecule have generally been drawn in a parallel configuration, with the carboxyl termini at one end, linked by a disulfide bond, and the amino termini at the other. This representation was no doubt chosen for convenience (the drawing is more compact) and for lack of any contrary evidence. The evidence presented here suggests that each polypeptide chain spans only one half the strand; their carboxyl termini are joined in the center of the strand and the amino termini are at the ends (Fig. 6).

The strongest evidence supporting this model is our determination of the length of the plasmic fragments. In the parallel chain molecule each of the 220,000 mol wt chains would span the entire 160-nm length, so the 190,000 mol wt fragments should be reduced in length correspondingly, to 140 nm. In the alternative model (Fig. 6) the 220,000 mol wt native chain spans only half the strand (80 nm) and the 190,000 mol wt fragment should be 70 nm long. The 65-nm length measured for this fragment corresponds closely to this model.

One of the most remarkable structural characteristics of fibronectin is its extreme flexibility. Both the bending and the length variation of fibronectin may be due to a single mechanism of flexibility in tertiary structure at points along the strand. These points of flexibility might be fixed segments of flexible polypeptide chain that alternate with segments of compact and rigid tertiary structure. To be consistent with our observations, the compact domains in this type of permanent nodular model would have to be quite small, producing an apparently uniform strand of 2-nm Diam. Alternatively, the points of flexibility might be produced transiently by denaturation and uncoiling at many, or perhaps all, points along the strand. This might be possible if the polypeptide chain were

coiled into a weakly bonded structure along most of its length. It is important to emphasize that, apart from the mechanism for flexibility, the molecule is not a random polypeptide chain but must be coiled or folded into the well-defined structure we have visualized.

The fibronectin strands are strikingly similar in appearance to actin binding protein and filamin, which have been studied by other groups (7, 20). The two subunits of actin binding protein are somewhat larger than those of fibronectin (270,000 versus 220,000 mol wt) and the average length is correspondingly greater. The electron micrographs show the same flexibility for bending, and the similarity of the sedimentation coefficients, 9.4S for actin binding protein (7) and 10S for fibronectin, confirms that they have a similar conformation in solution. Finally, both molecules show a distribution of lengths, actin binding protein varying from 120 to 190 nm (7) and fibronectin varying from 120 to 160 nm.

A major function of both fibronectin and actin binding protein is to form attachments to the actin cables of the cytoskeleton. Actin binding protein, which is a cytoplasmic protein, binds the actin cables to each other to form an integrated cytoskeleton. The points of attachment of fibronectin to the cell surface correspond to the location of actin cables in the cytoplasm (8, 18). Thus fibronectin attaches the cytoskeleton to the extracellular matrix. An intriguing observation is that fibronectin has a binding affinity for actin (9). To conclude that fibronectin may be a transmembrane protein, with a cytoplasmic segment that binds to the actin cables, is, however, speculative and perhaps premature. There is evidence that this attachment may be mediated by a third protein (2, 19).

The very similar structural characteristics of fibronectin and actin binding protein, both of which are long, highly flexible strands, may reflect their similar functional roles: anchoring the actin cables of the cytoskeleton to each other in one case and to the extracellular matrix in the other. In both cases the crosslinking molecules have to be long enough to bridge the attachment sites and sufficiently flexible to maintain the attachments to the dynamically changing and motile cytoskeleton.

We thank Claudene Paschal for excellent technical assistance in the preparation of fibronectin and the proteolytic fragments. J. McDonagh is an established investigator of the American Heart Association.

This work was supported by National Heart, Lung, and Blood Institute grants 21139, 22505, and 23454.

Received for publication 20 April 1981, and in revised form 30 July 1981.

REFERENCES

1. Alexander, S., G. Colonna, and H. Edelhoch. 1979. The structure and stability of human plasma cold-insoluble globulin. *J. Biol. Chem.* 254:1501–1505.
2. Burridge, K., and J. R. Feramisco. 1980. Microinjection and localization of a 130K protein in living fibroblasts: a relationship to actin and fibronectin. *Cell.* 19:587–595.
3. Elliott, A., and G. Offer. 1978. Shape and flexibility of the myosin molecule. *J. Mol. Biol.* 123:505–519.
4. Engvall, E., E. Ruoslahti, and E. Miller. 1978. Affinity of fibronectin to collagens of different genetic types and to fibrinogen. *J. Exp. Med.* 147:1584–1595.
5. Fowler, W., and H. Erickson. 1979. Trinodular structure of fibrinogen—confirmation by both shadowing and negative stain electron microscopy. *J. Mol. Biol.* 134:241–249.
6. Fowler, W., H. Erickson, R. Hantgan, J. McDonagh, and J. Hermans. 1981. Cross-linked fibrinogen dimers demonstrate a feature of the molecular packing in fibrin fibers. *Science (Wash. D. C.).* 211:287–289.
7. Hartwig, J., and T. Stossel. 1981. Structure of macrophage actin-binding protein molecules in solution and interacting with actin filaments. *J. Mol. Biol.* 145:563–581.
8. Hynes, R., and A. Destree. 1978. Relationships between fibronectin (LETS protein) and actin. *Cell.* 15:875–886.
9. Keski-Oja, J., A. Sen, and G. Todaro. 1980. Direct association of fibronectin and actin molecules in vitro. *J. Cell Biol.* 85:527–533.
10. Koteliansky, V. E., M. V. Bejanian, and V. N. Smirnov. 1980. Electron microscopy study of fibronectin structure. *FEBS (Fed. Eur. Biochem. Soc.) Lett.* 120:283–286.
11. Kurkinen, M., T. Vartio, and A. Vaheri. 1980. Polypeptides of human plasma fibronectin are similar but not identical. *Biochim. Biophys. Acta.* 624: 490–498.
12. McDonagh, J., H. Messel, R. P. McDonagh, G. Murano, and B. Blomback. 1972. Molecular weight analysis of fibrinogen and fibrin chains by an improved SDS gel electrophoresis method. *Biochim. Biophys. Acta.* 257:135–142.
13. McDonagh, R. P., J. McDonagh, T. Petersen, H. Thøgersen, K. Skorstengaard, L. Sottrup-Jensen, and S. Magnusson. 1981. Amino acid sequence of the Factor XIIIa acceptor site in bovine plasma fibronectin. *FEBS (Fed. Eur. Biochem. Soc.) Lett.* 127:174–178.
14. Mosher, D. 1980. Fibronectin. *Prog. Hemostasis Thromb.* 5:111–150.
15. Mosher, D., P. Schad, and J. Vann. 1980. Cross-linking of collagen and fibronectin by Factor XIIIa: localization of participating glutaminyl residues to a tryptic fragment of fibronectin. *J. Biol. Chem.* 255:1181–1188.
16. Ruoslahti, E., E. Engvall, and E. Hayman. 1981. Fibronectin: current concepts of its structure and functions. *Collagen Research.* 1:95–128.
17. Shotton, D., B. Burke, and D. Branton. 1979. The molecular structure of human erythrocyte spectrin. *J. Mol. Biol.* 131:303–329.
18. Singer, I. 1979. The fibronexus: a transmembrane association of fibronectin-containing fibers and bundles of 5 nm microfilaments in hamster and human fibroblasts. *Cell.* 16: 675–685.
19. Singer, I., and P. Paradiso. 1981. A transmembrane relationship between fibronectin and vinculin (130 kd protein). *Cell.* 24:481–492.
20. Tyler, J., J. Anderson, and D. Branton. 1980. Structural comparison of several actin-binding macromolecules. *J. Cell Biol.* 85:489–495.
21. Tyler, J., and D. Branton. 1980. Rotary shadowing of extended molecules dried from glycerol. *J. Ultrastruct. Res.* 71:95–102.
22. Vaheri, A., and D. Mosher. 1978. High molecular weight, cell surface-associated glycoprotein (fibronectin) lost in malignant transformation. *Biochim. Biophys. Acta.* 516:1–25.
23. Vuento, M., T. Vartio, M. Saraste, C. von Bonsdorff, and A. Vaheri. 1980. Spontaneous and polyamine-induced formation of filamentous polymers from soluble fibronectin. *Eur. J. Biochem.* 105:33–42.
24. Wagner, D., and R. Hynes. 1980. Topological arrangement of the major structural features of fibronectin. *J. Biol. Chem.* 255:4304–4312.
25. Wrigley, N. 1968. The lattice spacing of catalase as an internal standard of length in electron microscopy. *J. Ultrastruct. Res.* 24:454–464.
26. Yamada, K., and K. Olden. 1978. Fibronectins—adhesive glycoproteins of cell surface and blood. *Nature (Lond.).* 275:179–184.